



Synthesis of double-hydrophilic antiscalant and evaluation of its CaCO_3 , CaSO_4 and $\text{Ca}_3(\text{PO}_4)_2$ precipitation performance

Tiantian Wang^a, Yuming Zhou^{a,*}, Qingzhao Yao^{a,*}, Jun Li^a, Ao Zhang^a, Yiyi Chen^a, Xiangnan Chen^b, Qiuli Nan^b, Mingjue Zhang^b, Wendao Wu^c, Wei Sun^c

^aSchool of Chemistry and Chemical Engineering, Southeast University, Nanjing 211189, China, Tel. +86-25-52090617; email: ymzhou@seu.edu.cn (Y. Zhou), Tel. +86-25-52090617; email: 101006377@seu.edu.cn (Q. Yao), Tel. +86-25-52090617; email: xywangtiantian77@163.com (T. Wang), Tel. +86-25-52090617; email: 1543107327@qq.com (J. Li), Tel. +86-25-52090617; email: 807543700@qq.com (A. Zhang), Tel. +86-25-52090617; email: 838331357@qq.com (Y. Chen)

^bCheng Xian College, Southeast University, Nanjing 210088, China, Tel. +86-25-52090617; email: 528538371@qq.com (X. Chen), Tel. +86-25-52090617; email: 53212651@qq.com (Q. Nan), Tel. +86-25-52090617; email: 489354839@qq.com (M. Zhang)

^cJianghai Environmental Protection Co., Ltd, Changzhou 213116, Jiangsu, China, Tel. +86-25-52090617; email: 13887303@qq.com (W. Wu), Tel. +86-25-52090617; email: leojhgh@sina.com (W. Sun)

Received 3 September 2016; Accepted 16 February 2017

ABSTRACT

A non-phosphorus copolymer, acrylic acid-isoprenyl polyethoxy carboxylate copolymer (AA-TPEL) is synthesized and employed as a multifunctional scale inhibitor for calcium carbonate, calcium sulfate and calcium phosphate deposits. The molecular structure of TPEL and AA-TPEL is characterized by Fourier transform infrared spectroscopy and ¹hydrogen nuclear magnetic resonance spectroscopy. Scanning electron microscopy (SEM) and X-ray powder diffraction are used to characterize the surface morphology and crystal form of calcium scales. Compared with several current commercial inhibitors, AA-TPEL exhibits excellent ability to control calcium precipitation, with approximately 88.67% CaCO_3 inhibition and 97.07% CaSO_4 inhibition at levels of 8 and 3 mg L⁻¹, respectively. It also maintain superior ability to prevent the formation of $\text{Ca}_3(\text{PO}_4)_2$ scale with 98.92% inhibition efficiency at the low level of 4 mg L⁻¹. The inhibitory behavior of the polymer is determined by using static scale inhibition method.

Keywords: Antiscalant; Multifunctional copolymer; Calcium scales; Mechanism

1. Introduction

Scale deposition is a universal phenomenon existing in recirculating cooling water systems [1]. Some mineral salts exhibit inverse solubility characteristics, as the temperature rises, the solubility decreases [2]. Consequently, with the increase of iterations, severe scale deposition problems will be caused by the elevated water temperature and ion concentrations.

Consequently, the high water temperature and elevated ion concentration could lead to severe scale deposition problems as the number of iterations increased [3]. Among which, calcium carbonate (CaCO_3), calcium sulfate (CaSO_4) and

calcium phosphate ($\text{Ca}_3(\text{PO}_4)_2$) scales are the most prone to be encountered [4]. The deleterious effects cannot be swallowed because the generated scales could cause technical and economic problems such as reduced cooling efficiency, increased pipeline cleaning costs, even scheduled and unscheduled shutdowns. Thus, choosing a kind of effective method to suppress precipitation is of great importance both in industry and academia [3,5–7]. Chemical additives known for their strong ability of complexation with ions and superior dispersion peculiarity play a major role to control the formation of scales [6,8].

Polycarboxylate and polyphosphonate are the most widely used and effective scale inhibitors of calcium scales. The polyphosphonate is highly unstable in aqueous solution;

* Corresponding author.

they hydrolyze, end up as ineffective orthophosphate, and as a result cause secondary pollution and induce severe challenges to water treatment plants as well as the environment. Another frequently used inhibitor is polycarboxylate, which has a low calcium tolerance and will react with calcium ions to form insoluble calcium-polymer salts [9–12]. Thus, phosphorous-free and less toxic scale inhibitors with the capacity of preventing CaCO_3 , CaSO_4 and $\text{Ca}_3(\text{PO}_4)_2$ scales have become an imperative focus to water treatment technology.

Our laboratory has developed a series of phosphate- and nitrogen-free scale inhibitors (APEC_n, APEL_n, allyloxy polyethoxy ether (monochloroacetic acid-allyl polyethoxy carboxylate (APEG)-glycidol (PG)\COOH, oxalic acid-allyl polyethoxy carboxylate (APEM_n)) by the copolymerization of modified polyether with other monomers. However, all of them are based on the APEG. Owing to the retardation of allyloxy during polymerization, APEG in the choice of comonomer is intensively limited [13,14]. In addition, the double bond of allyloxy is vulnerable to heat, and then rearrangement reaction occurred that lead to the polymerization activity of double bond depressed.

As a contribution to the endeavor to eliminate the negative impact, a novel type of copolymer with multifunctional property and excellent copolymerization ability is developed. Recently, a burgeoning macromolecule polymer made from isoprenyl oxy poly(ethylene glycol) (TPEG) has become very active because of its easily preparation from versatile raw materials and its high effectiveness [15]. The reason is that TPEG is not merely exist eminent copolymerization with other monomers but also maintain an eminent conversion rate [14]. Besides, the market price of isoprenyl polyethoxy carboxylate copolymer (TPEL) is cheaper than APEG, and there is no report of scale inhibitor synthesized by TPEG in cooling water systems.

On the basis of the reasons mentioned above, this work forms part of ongoing research projects aiming to synthesize an environment-friendly double-hydrophilic polymer called acrylic acid-isoprenyl polyethoxy carboxylate copolymer (AA-TPEL) to inhibit the calcium scales in cooling water systems. The large number of carboxylate functional groups (–COO–) act as anchor blocks, which interact with the substrate, and the hydrophilic polyethylene glycol (PEG) block, which renders enhanced solubility [7].

2. Experimental setup

2.1. Materials

TPEG (with M_n number (average molecular weight) 2,400 g mol^{-1}) was purchased from Shanghai Taijie Chemical, China. All other reagents, such as acrylic acid (AA), succinic anhydride (SA), ammonium persulfate (APS), calcium chloride (CaCl_2), sodium bicarbonate (NaHCO_3), sodium sulfate (Na_2SO_4), potassium phosphate monobasic (KH_2PO_4), borax ($\text{Na}_2\text{B}_4\text{O}_7 \cdot 10\text{H}_2\text{O}$) and ethylenediaminetetraacetic acid (EDTA), were of analytical reagent grade and obtained from Zhongdong Chemical Reagent (Nanjing, Jiangsu, China) and were used as received without further purification. The commercial inhibitors of poly(epoxysuccinic acid) (PESA, M_w weight (average molecular weight) 1,500), ethylenediaminetetramethylenephosphonic acid (EDTMP, 436 M_w) and 1-hydroxyethylidene-1,1-diphosphonic acid (HEDP, 206 M_w)

were of technical grade and were supplied by Jiangsu Jianghai Chemical Co., Ltd. Distilled water was used for all the studies.

2.2. Measurements

FTIR spectroscopy (VECTOR-22, Bruker Co., Germany) was used to characterize the presence of expected functional groups. The pellets were prepared by pressing the mixture of the samples and potassium bromide powder. ^1H NMR spectra were performed on a 400 MHz spectrometer (AVANCE AV-500, Bruker, Switzerland) with dimethyl sulfoxide- d_6 (DMSO- d_6) as the solvent. The surface morphology and the size changes of CaCO_3 and CaSO_4 were explored by a field emission scanning electron microscope (S-3400N Hitachi SEM). The X-ray powder diffraction (XRD) patterns were conducted by using a D-8 powder X-ray diffractometer with Cu $K\alpha$ radiation (40 kV, 40 mA). Besides, angle range ranging from 5° and 70° was selected to analyze the crystal structure.

2.3. Preparation of TPEL and AA-TPEL

The carboxylic acid functionalization of the surface hydroxyl groups was realized by reaction with SA; the synthesis procedure of TPEL is shown in Fig. 1. AA-TPEL copolymer was prepared from TPEL and AA through free radical polymerization according to the procedure as follows: a four-neck round bottom flask, equipped with a thermometer and a magnetic stirrer, was filled with 40 mL of deionized water and TPEL under nitrogen atmosphere. APS was used as initiator. When the temperature rose to 70°C , APS, AA aqueous solution was added into the reaction mixture dropwise and separately for 1.5–2 h, and then heated to 80°C and maintained at the temperature additionally for 3 h. Finally, the colorless transparent liquid product AA-TPEL was obtained, with approximately 20% solid content. The preparation procedure of AA-TPEL is shown in Fig. 2.

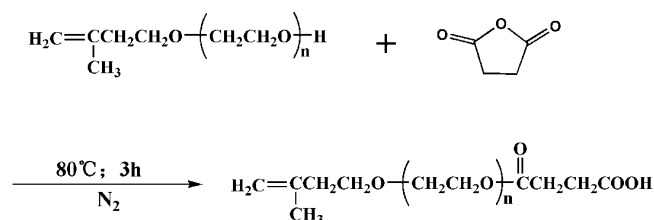


Fig. 1. Preparation of TPEL.

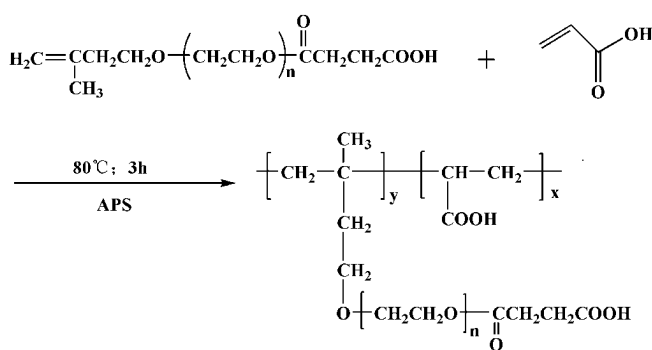


Fig. 2. Preparation of AA-TPEL.

2.4. Standard precipitation of CaCO_3 , CaSO_4 and $\text{Ca}_3(\text{PO}_4)_2$ experiments

The precipitation of CaCO_3 experiments were carried out in flask test and followed the standard of People's Republic of China (GB/T 16632–2008). It should be noted that all chemical scales inhibitor dosages given below were considered on a basis of dried conditions obtained from AA-TPEL. The CaCl_2 (0.15 mol L^{-1}) and NaHCO_3 (0.3 mol L^{-1}) and borax buffer solution should be prepared in advance, and then kept in volumetric flask at room temperature. Calcium carbonate precipitation and inhibition was studied in artificial cooling water, which was prepared by mixing a certain quantity (20 mL) of each prepared solution of CaCl_2 and NaHCO_3 with deionized water. The final concentration of Ca^{2+} and HCO_3^- was 240 and 732 mg L^{-1} , respectively, with the solution pH 9 adjusting by borax buffer solution. Each inhibition test was carried out in a flask of 500 mL capacity immersed in a temperature-controlled bath for 10 h at 80°C ; then filtrate was collected ($0.22 \mu\text{m}$) to measure the Ca^{2+} concentration. All Ca^{2+} ions concentration remaining in the solutions were titrated by EDTA standard solution. Calconcarboxylic acid was used as indicator; when the color of the solution changes from violet to bright blue, the end point of titration reached. Inhibitor efficiency was calculated from the following equation:

$$\text{Inhibition (\%)} = \frac{[\text{Ca}^{2+}]_{\text{final}} - [\text{Ca}^{2+}]_{\text{blank}}}{[\text{Ca}^{2+}]_{\text{initial}} - [\text{Ca}^{2+}]_{\text{blank}}} \times 100\% \quad (1)$$

where $[\text{Ca}^{2+}]$ is the concentration of Ca^{2+} ions. The $[\text{Ca}^{2+}]_{\text{final}}$ and $[\text{Ca}^{2+}]_{\text{blank}}$ are the filtrates obtained after the calcium carbonate supersaturated solutions heated for 10 h at 80°C , containing and not containing scale inhibitor, respectively. And $[\text{Ca}^{2+}]_{\text{initial}}$ is the concentration of Ca^{2+} ions at the beginning of the experiment.

Calcium sulfate precipitation experiments were carried out according to the national standard of People's Republic of China concerning the code for the design of industrial oil field-water treatments (SY/T 5673-93). Procedure of experiments used for calcium carbonate is also available to calcium sulfate precipitation experiments, except that the CaCl_2 and Na_2SO_4 concentrations are $6,800 \text{ mg L}^{-1}$ Ca^{2+} and $7,100 \text{ mg L}^{-1}$ SO_4^{2-} , respectively. It is noteworthy that before mixing with Na_2SO_4 solutions, chemical inhibitors should be added to the CaCl_2 solutions ahead. Then the solution was still reacted in a temperature-controlled bath at 70°C for 6 h, and the determination of Ca^{2+} was done by exactly same process as CaCO_3 . The inhibition efficiency of AA-TPEL against calcium sulfate scale was calculated as Eq. (1).

Calcium phosphate precipitation experiments were carried out using solutions of CaCl_2 (100 mg L^{-1} Ca^{2+}), KH_2PO_4 (5 mg L^{-1} PO_4^{3-}) according to the national standard of People's Republic of China (GB/T 22626-2008). The solution in a flask of 500 mL capacity was still reacted in a temperature-controlled bath at 80°C for 10 h, and then collected the filtered ($0.22 \mu\text{m}$) solution to calculate phosphate concentration. Instead of using EDTA complexometry titration, the determination of PO_4^{3-} concentration was evaluated

under the wavelength of 710 nm with 722-spectrophotometer by absorbance (GBT 6913-2008). The inhibition efficiency of AA-TPEL against calcium phosphate scale was calculated as follows (Eq. (2)):

$$\text{Inhibition (\%)} = \frac{[A]_{\text{final}} - [A]_{\text{blank}}}{[A]_{\text{initial}} - [A]_{\text{blank}}} \times 100\% \quad (2)$$

where $[A]_{\text{final}}$ is the absorbance of phosphate in the filtrate in the presence of inhibitors at 10 h; $[A]_{\text{blank}}$ is the absorbance of phosphate in the filtrate in the absence of inhibitors at 10 h; and $[A]_{\text{initial}}$ is the absorbance of phosphate at the beginning of the experiment.

3. Results and discussion

3.1. FTIR analysis of the copolymer

The FTIR spectra record for the synthesized TPEG (a), TPEL (b) and AA-TPEL (c) polymers are presented in Fig. 3. There is a strong absorption peak at $3,440 \text{ cm}^{-1}$ assigned to the stretching vibration of O–H. The band at $1,104 \text{ cm}^{-1}$ is from the stretching vibration of C–O–C group. The peak observed at $1,644 \text{ cm}^{-1}$ is due to the stretching vibration of C=C group (a). The strong absorption peak at $1,740 \text{ cm}^{-1}$ in curve (b) is associated with the stretching vibration of C=O. It reveals clearly that TPEL has been synthesized successfully. The peak at $1,644 \text{ cm}^{-1}$ that appears in curves (a) and (b) but disappears completely in curve (c) proves that copolymerization between AA and TPEL has happened.

3.2. $^1\text{HNMR}$ analysis of the copolymers

Further characterization, $^1\text{HNMR}$, was performed to confirm this structure. $^1\text{HNMR}$ spectra of TPEG (a), TPEL (b) and AA-TPEL (c) are shown in Fig. 4.

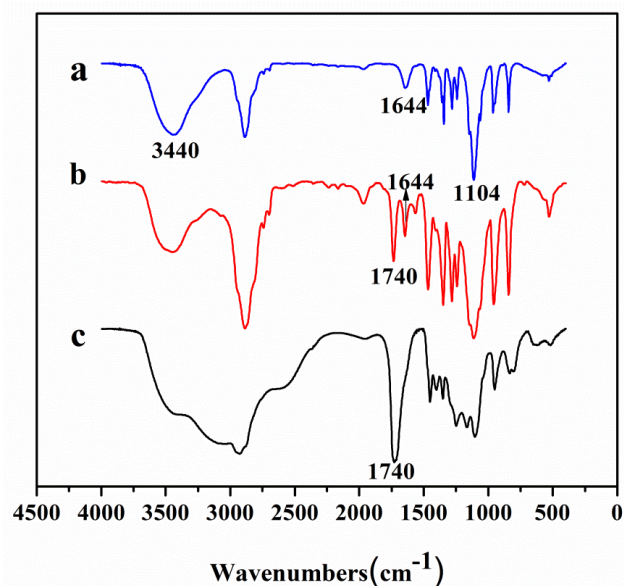


Fig. 3. FTIR spectrum of TPEG (a), TPEL (b) and AA-TPEL (c).

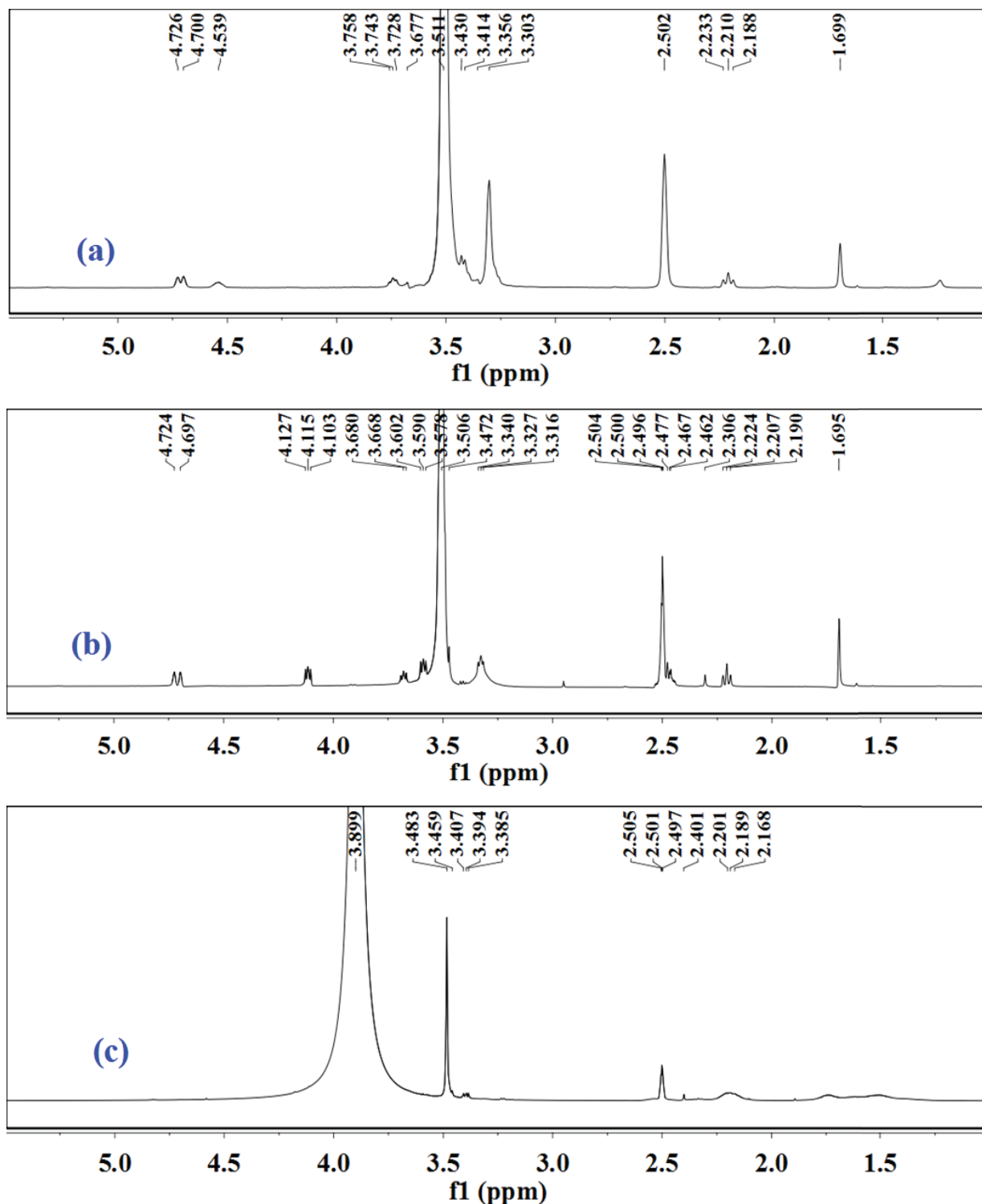


Fig. 4. ^1H NMR spectrum of TPEG (a), TPEL (b) and AA-TPEL (c).

- TPEG (Fig. 4(a); 400 MHz, DMSO- d_6 , δ ppm): 1.69–1.70 ($-\text{CH}_3$, methyl proton), 2.18–2.23 ($-\text{CH}_2-$, methylene proton), 2.50 (solvent residual peak of DMSO), 3.40–3.70 ($-\text{CH}_2\text{CH}_2\text{O}-$, ether groups), 4.40–4.60 ($-\text{OH}$, active hydrogen in TPEG) and 4.68–4.76 ($\text{CH}_2=$, methyl propenyl protons).
- TPEL (Fig. 4(b); 400 MHz, DMSO- d_6 , δ ppm): 1.69–1.70 ($-\text{CH}_3$, methyl protons), 2.17–2.25 ($-\text{CH}_2-$, methylene proton), 2.30–2.51 ($-\text{CH}_2\text{CH}_2-$, protons in $-\text{COCH}_2\text{CH}_2\text{COOH}$), 2.50 (solvent residual peak of DMSO), 3.40–3.60 ($-\text{CH}_2\text{CH}_2\text{O}-$, ether groups), 4.70–4.73 ($\text{CH}_2=$, methyl propenyl protons) and 4.10–4.15 ($-\text{COOCH}_2-$, ester protons).

- AA-TPEL (Fig. 4(c); 400 MHz, DMSO- d_6 , δ ppm): 2.16–2.21 (–CH₂–, methylene proton), 2.30–2.51 (–CH₂CH₂–, protons in –COCH₂CH₂COOH), 2.50 (solvent residual peak of DMSO) and 3.40–3.60 (–CH₂CH₂O–, ether groups).

Compared with Figs. 4(a) and (b), the entire disappearance of δ 4.40–4.60 ppm (–OH, active hydrogen in TPEG) in Fig. 4(a) and appearance of δ 4.10–4.25 ppm (–COOCH₂–, ester protons) and δ 2.30–2.51 (–CH₂CH₂–, protons in –COCH₂CH₂COOH) in Fig. 4(b) prove that TPEL has been synthesized. Meanwhile, δ 4.68–4.76 ppm (CH₂=, methyl propenyl protons) attributed to double bond absorption peak completely disappeared in Fig. 4(c) reveals that free radical polymerization among AA and TPEL has been successfully realized. From FTIR and ¹HNMR analysis, it can conclude that synthesized AA-TPEL corresponds directly with anticipated structure.

3.3. Effect of inhibitor on calcium scales

The scale inhibition rate of calcium carbonate, calcium sulfate and calcium phosphate as a function of polymer concentration is shown in Figs. 5–7. The dosage and molar ratio of AA/TPEL copolymer has a strong impact on the formation of calcium scales precipitation. All of the CaCO₃, CaSO₄ and Ca₃(PO₄)₂ inhibition exist an obvious “threshold effect”, namely the scale inhibition efficiency increased slowly with the increasing of copolymer concentration [1]. The threshold scale of inhibition of the polymers is due to their adsorption on the growing crystal phases of the nuclei, which results in the distortion and retardation of the crystal growth [16].

3.3.1. Effect of inhibitor on CaCO₃ scale

As can be seen from Fig. 5, the scale efficiency rises with the increase of copolymer concentration from 2 to 8 mg L⁻¹. At 2 mg L⁻¹ dosage, the polymer shows poor calcium carbonate inhibition; however, at 8 mg L⁻¹, the performance of the

polymer is substantially improved and then keeping steady level. Besides, the CaCO₃ scale inhibition efficiency of different molar ratio is observed to decrease in the order: 2:1 (AA/TPEL, mole ratio) > 3:1 > 1:1 > 1:2, and the antiscaling efficiency of AA/TPEL (2:1) reaches to 88.67% at the threshold concentration. Therefore, the molar ratio of 2:1 (AA/TPEL) is the optimum proportion to inhibit calcium carbonate scales.

3.3.2. Effect of inhibitor on CaSO₄ scale

The mitigation ability of AA-TPEL of the polymer on CaSO₄ scale is presented in Fig. 6. It can be observed that the CaSO₄ scale inhibition efficiency is significantly affected by the dosage of AA-TPEL. The inhibition efficiency is only 39.21% with 1 mg L⁻¹. Whereas, there is a rapid increase of scale inhibition as the concentrations range from 1 to 3 mg L⁻¹. Under the same experimental conditions, the inhibition efficiency is achieved with the molar ratio AA/TPEL (3:1), which is about 97.07% at a level of 3 mg L⁻¹. However, AA/TPEL (1:1), AA/TPEL (2:1) and AA/TPEL (1:2) exist only up to 65.96%, 83.21% and 46.17% CaSO₄ scale inhibition efficiency, respectively. Hence, the molar ratio of 3:1 (AA/TPEL) is chosen for further experiments.

3.3.3. Effect of inhibitor on Ca₃(PO₄)₂ scale

The line graph presented in Fig. 7 indicated that concentration and mole ratio have significant influence on the mitigation ability of AA-TPEL. The different molar ratio of copolymers lead to different inhibition efficiency toward Ca₃(PO₄)₂ scales. In spite of the disparity in critical concentration of different mole ratios, the scale inhibition efficiency of 100% could be achieved finally. According to the data, the copolymers achieve superior efficiency about 98.92% on Ca₃(PO₄)₂ inhibition at the mole ratio 1:1 with the critical value of 4 mg L⁻¹; however, the threshold concentration of the other mole ratio AA/TPEL (1:2), AA/TPEL (2:1) and AA/TPEL (3:1) exist up to 8, 9 and 10 mg L⁻¹, respectively. The large number of carboxylate functional groups in the copolymer

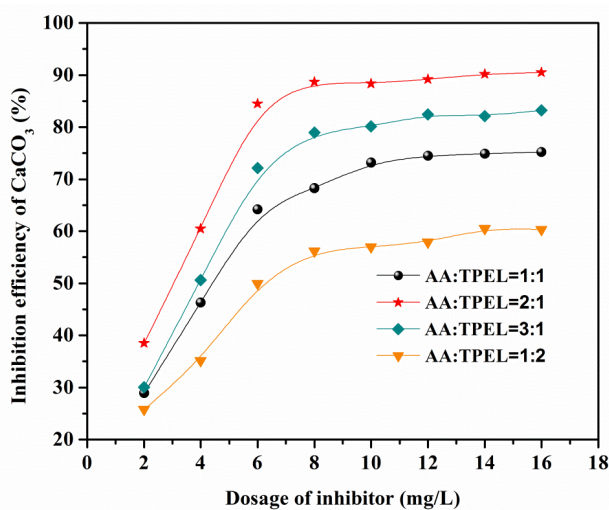


Fig. 5. The influence of the dosage and mole ratio on the inhibition of CaCO₃.

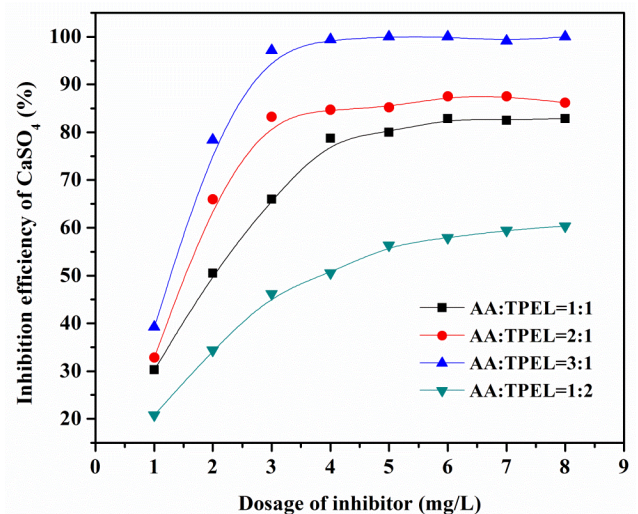


Fig. 6. The influence of the dosage and mole ratio on the inhibition of CaSO₄.

structure act as anchor blocks, which can help the copolymer more accessible and easily interact with the surface of crystals; the polyethylene glycol (PEO) blocks are not expected to exhibit any affinity for $\text{Ca}_3(\text{PO}_4)_2$ and act as a hydrophilic stabilizer and have the potential to keep steric and electrostatic repulsion of the blocks [17]. Therefore, the balance between AA and isoprenyl polyethoxy carboxylate carry the status to get optimum effect.

3.4. Comparison of calcium scales inhibition efficiency

The most appropriate molar ratio (AA/TPEL) of the copolymer to inhibit calcium carbonate, calcium sulfate and calcium phosphate scales formation is 2:1, 3:1 and 1:1, respectively. The proportion is used in the further experiments. In order to have a better understanding of the copolymer, the ability of AA-TPEL to control calcium scales compared with EDTMP, HEDP and PESA are shown in Figs. 8–10, respectively.

3.4.1. Comparisons of CaCO_3 inhibition efficiency

Fig. 8 presents the evolution of the inhibition efficiency in artificial cooling water containing AA-TPEL and several other commercial inhibitors. As can be seen from Fig. 6, the ability to control calcium carbonate precipitation follow the order AA-TPEL > EDTMP > HEDP > PESA. AA-TPEL shows great potential at the threshold concentration for calcium carbonate inhibition compared with the commercial water treatment agents. This behavior gives the credit to the side-chain PEG segments of TPEL and carboxyl groups of AA, which play an important role during the control of calcium carbonate scales.

3.4.2. Comparisons of CaSO_4 inhibition efficiency

In this work, we also studied the influence of these inhibitors on the prevention of calcium sulfate scales as shown in Fig. 9. It is indicated that the order of preventing the precipitation of CaSO_4 is AA-TPEL > EDTMP > PESA > HEDP.

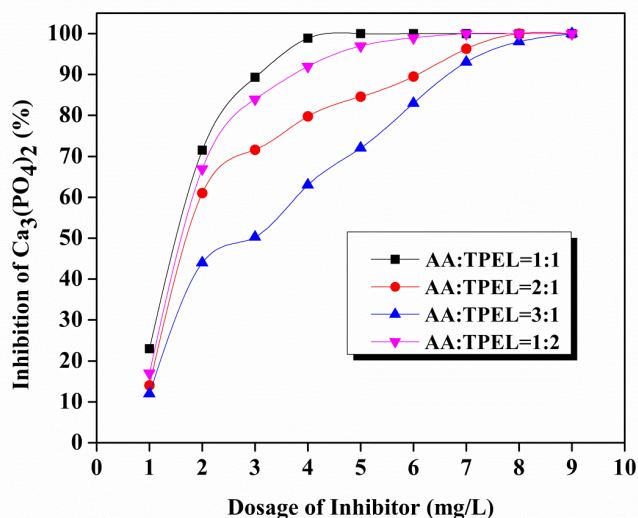


Fig. 7. The influence of dosage and mole ratio on the inhibition of $\text{Ca}_3(\text{PO}_4)_2$.

The inhibition efficiency of AA-TPEL reaches 97.07% at a level of 3 mg L^{-1} , however it is only 70.42% for EDTMP, 35.13% for PESA and 26.11% for HEDP, respectively, at the same dosage. It is worth mentioning that AA-TPEL has excellent ability to control not only calcium carbonate scales but also calcium sulfate scales at a low dosage.

3.4.3. Comparisons of $\text{Ca}_3(\text{PO}_4)_2$ inhibition efficiency

In the case of inhibitors, we notice that the capacity recorded in the presence of the inhibitors start at inferior values and then remain relatively elevator (Fig. 10). This phenomenon is observed with all inhibitors. It is worth mentioning that there is a sudden increase of scale inhibition for AA-TPEL as the concentration increase from 1 to 4 mg L^{-1} , the inhibition efficiency reaches up to 98.92% and finally 100% is achieved. Compared with commercial inhibitors, PESA,

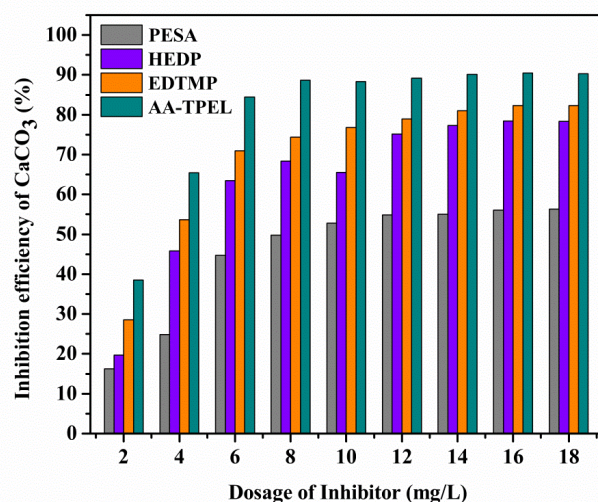


Fig. 8. Comparison of inhibition efficiency for CaCO_3 on calcium carbonate.

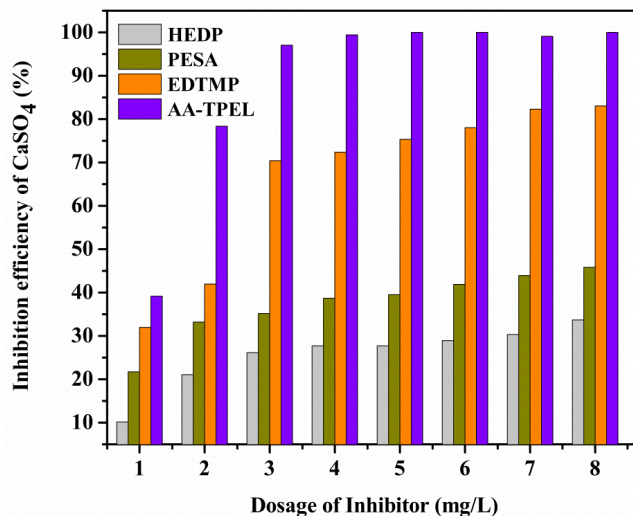


Fig. 9. Comparison of inhibition efficiency for CaSO_4 on calcium carbonate.

EDPMP and HEDP, the ability to control calcium phosphate precipitation is AA-TPEL > HEDP > EDTMP > PESA; the copolymers AA-TPEL exhibited excellent properties to inhibit $\text{Ca}_3(\text{PO}_4)_2$ scales.

3.5. Morphology characterization of calcium scales

3.5.1. SEM studies

The morphology of collected CaCO_3 and CaSO_4 scales in the absence and the presence of copolymer are characterized by means of a scanning electron microscopy (SEM). The results are presented in Figs. 11 and 12. As shown in Fig. 11(a), in the absence of the AA-TPEL copolymer, the particles of precipitated CaCO_3 present well-developed rhombohedral morphology, with sharp, straight edges. In contrast, obvious change is noted when copolymer is added. It can be seen from Figs. 11(b)–(d), the crystals are destroyed and crumbled when the dosage of copolymer is only 2 mg L⁻¹ (b), when the concentration is 4 mg L⁻¹, oblate spherical shape particles

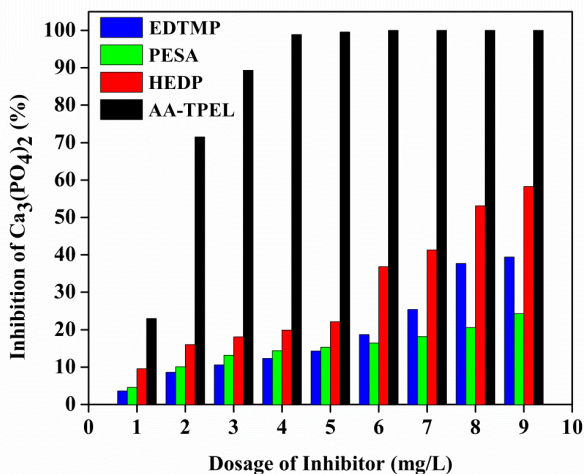


Fig. 10. Comparison of inhibition efficiency on $\text{Ca}_3(\text{PO}_4)_2$.

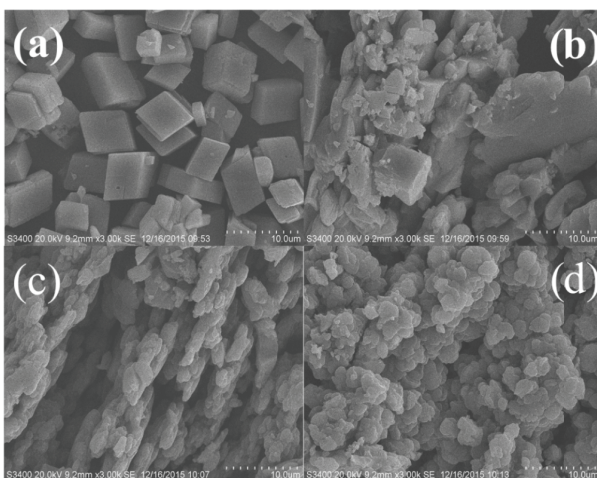


Fig. 11. SEM images of calcium carbonate crystals: in the absence of AA-TPEL (a) and in the presence of AA-TPEL: (b) 2 mg L⁻¹, (c) 4 mg L⁻¹ and (d) 8 mg L⁻¹.

come into view (c), as the concentration increase to 8 mg L⁻¹, the morphology turned into layer structures (d). With the concentration of the polymer ranging from 2 to 8 mg L⁻¹, CaCO_3 gradually loses its sharp edges, and the morphology is transformed from the cubic forms to the smaller fragments. Recently, it has been found that the precipitation of CaCO_3 with varying copolymer concentrations always resulted in phase pure crystalline samples for one of the three different polymorphs [18]. Therefore, the different morphology may correspond with the microstructure of calcium carbonate, calcite (a), aragonite (c), and vaterite (d). Consequently, the lattice distortion occurs in the presence of copolymer, and the crystal morphology is then changed [19].

A significant change in the morphology and size of the calcium sulfate scale is shown in the micrograph presented in Fig. 12. The micrograph in Fig. 12(a) shows that calcium sulfate crystals are in regular rod shape with monoclinic and prismatic structures in the absence of inhibitor. While in Fig. 12(b) with the dosage of the copolymer just only 1 mg L⁻¹, the morphology has undergone tremendous changes. The sharp edges and acute corners of the crystals are destroyed seriously. When the AA-TPEL concentration increases to 3 mg L⁻¹, amorphous agglomerate and brittle material with no sharp edges is produced (Fig. 12(d)) [4]. Moreover, the fractured particles become the major morphology of the calcium sulfate, which means that the scale is floppy and can be removed easily.

3.5.2. XRD studies

XRD is used to examine the microstructure change of CaCO_3 , CaSO_4 and $\text{Ca}_3(\text{PO}_4)_2$ crystals, and the spectrogram for calcium carbonate is presented in Figs. 13–15. As shown in Fig. 13(a) in the absence of AA-TPEL, the diffraction peaks at 23.053°, 29.400°, 31.435°, 35.968°, 39.408°, 43.157°, 47.113°, 47.505°, 48.503°, 56.561° and 57.397° correspond to crystal faces 012, 104, 006, 110, 113, 202, 024, 018, 116, 121 and 122, respectively, typical of calcite. This indicates that calcite is the main crystal form in the absence of scale inhibitor. In the presence of scale inhibitor, strong peaks appeared at 21.004°,



Fig. 12. SEM images of calcium sulfate crystals: in the absence of AA-TPEL (a) and in the presence of AA-TPEL: (b) 1 mg L⁻¹, (c) 2 mg L⁻¹ and (d) 3 mg L⁻¹.

24.900°, 27.047°, 32.778°, 42.759°, 43.848°, 49.098°, 50.077° and 55.805° correspond to vaterite crystal faces 004, 110, 112, 114, 008, 300, 304, 118 and 224, respectively (Fig. 13(b)). Although there are still weak diffraction peak of 29.400°, the most stable morphology of calcite, however, the diffraction peak is greatly reduced or almost invisible. This indicates that vaterite morphs into the main crystal form in the presence of scale inhibitor.

Calcite, aragonite and vaterite are the three types of CaCO_3 crystal forms that are derived from amorphous calcium carbonate (ACC) [20]. It is found that calcite is the most thermodynamically stable; vaterite could be stabilized kinetically in the presence of the copolymer [21]. In other words, the scale inhibitor plays an important role in delaying the transformation from the less stable vaterite phase into the most stable calcite phase. Thus, XRD, combined with SEM analysis, illustrates AA-TPEL, which has a significant impact on the morphology and microstructure of calcium carbonate.

Additionally, the collected precipitate of CaSO_4 is identified by XRD, and the spectrogram is shown in Fig. 14. Calcium sulfate is reported to exist three crystallographic forms: calcium sulfate dihydrate form (gypsum), calcium sulfate hemihydrates (plaster of paris) and calcium sulfate anhydrite [22]. It is observed that in the absence of the AA-TPEL copolymer, gypsum ($\text{CaSO}_4 \cdot 2\text{H}_2\text{O}$) is the dominating crystal form of calcium sulfate (Fig. 14(a)). In another case, interplanar crystal spacing (d) and angle of intersection (θ) values of the spectrogram with copolymer still remain the same (Fig. 14(b)), that is, the addition of copolymer has shown no influence on the crystal structure but bring about changes in the morphology.

The majority of calcium phosphate deposits are amorphous in nature, whose main component is dicalcium phosphate dehydrate ($\text{CaHPO}_4 \cdot 2\text{H}_2\text{O}$, DCPD), and the most stable crystalline form is hydroxyapatite ($\text{Ca}_5(\text{PO}_4)_3\text{OH}$, HAP) [22,23]. As shown in Figs. 15(a) and (b), peak intensities decrease distinctly, especially at the diffraction peaks correspond to crystal faces 002 and 210, which means that the inhibitor shows the ability to retard the growth of apatite.

However, there are no significant changes of morphology for $\text{Ca}_3(\text{PO}_4)_2$ with the presence of AA-TPEL. It is reported that the solubility product (K_{sp}) of calcium phosphate is so small (2.07×10^{-33} (25°C)) that antiscaling should possess both scale inhibition and dispersion performance [24]. AA-TPEL is a kind of double-hydrophilic antiscalant, which is made up of PAA and PEO. Protonated carboxylate group is adsorbed to the surface of the inorganic particles, and the PEG, as a hydrophilic stabilizer, protects the particles from coagulation.

4. Inhibition mechanism

In this contribution, the polymerization mechanism is the free radical polymerization among AA and macromonomer. The scale-inhibition mechanism of AA-TPEL is discussed based on the current theories and measured consequences. The marked effect of polymers on calcium scales has been explained in terms of the following mechanisms such as: a multilayer type of adsorption on the scale surface, chelating solubilization, lattice distortion and electrostatic repulsion function [25].

SEM studies and XRD studies show that the morphology of CaCO_3 and CaSO_4 crystals has been dramatically changed

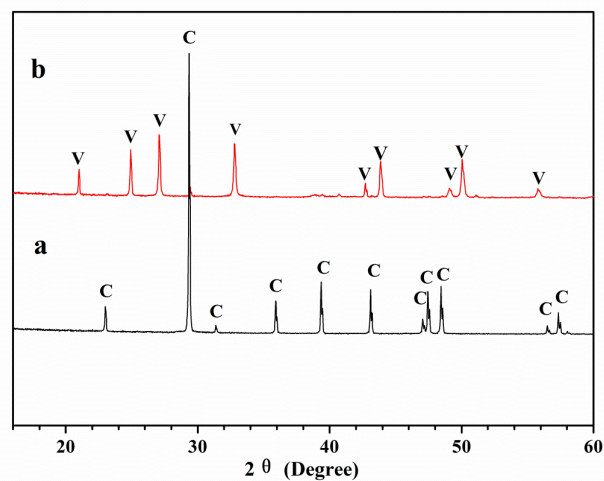


Fig. 13. XRD image of the CaCO_3 crystal: in the absence of AA-TPEL (a) and in the presence of AA-TPEL (b) 8 mg L^{-1} .

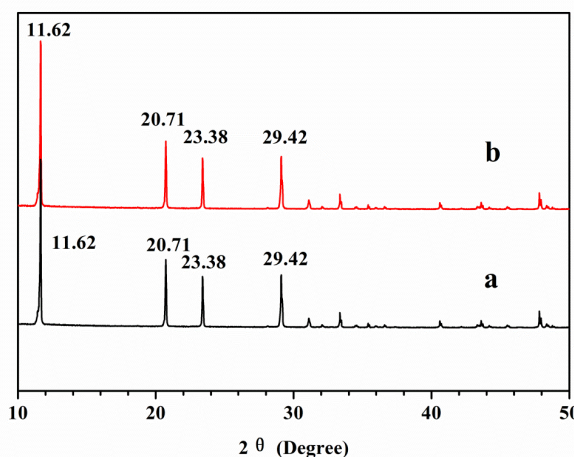


Fig. 14. XRD image of the CaSO_4 crystal: in the absence of AA-TPEL (a) and in the presence of AA-TPEL (b) 3 mg L^{-1} .

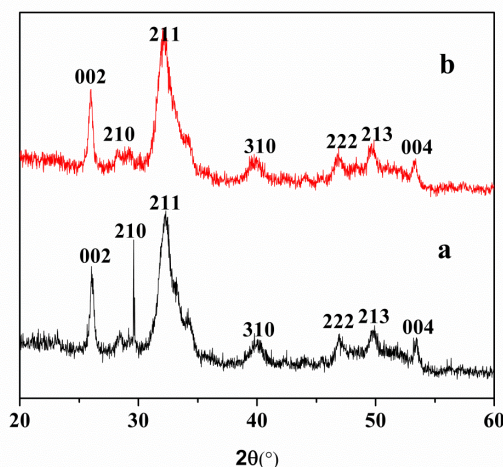


Fig. 15. XRD image of the $\text{Ca}_3(\text{PO}_4)_2$ crystal: in the absence of AA-TPEL (a) and in the presence of AA-TPEL (b) 4 mg L^{-1} .

by antiscalant. Both carboxylate ($-\text{COOH}$) and PEG segments of copolymer are hydrophilic blocks and exist randomly in water. A large amount of carboxylate functional groups increase the ionic attractive interactions between the adsorbate ($-\text{COO}^-$) and the positive sites (Ca^{2+}) through adsorption on the crystal surface, thus effectively reducing the number of active growth sites and result in lattice distortion, crystal fractures [26]. Although some of the growth sites of lower energy may still be free to grow, but they maintain a very slow rate. The polymer backbone then acts as a “fence” on the crystal surface, forming an obstacle for propagating steps that lead to further crystal growth. On the other hand, deprotonated carboxylate groups and calcium ions come into being the spontaneous formation of AA-TPEL–Ca complexes by dint of interaction or encapsulation, and the bonding strength has the ability to disorder the normal chemical structure of CaCO_3 and CaSO_4 , which contribute to dissolution of Ca^{2+} . At the same time, water-compatible PEG segments possess the very strong hydrophilicity, which not only increases its solubility in water but also results in steric and electrostatic repulsion. Therefore, the copolymer AA-TPEL possesses the ability to prevent $\text{Ca}_3(\text{PO}_4)_2$ minerals from precipitating through its superior ability to disperse solid particles. As a consequence, the random copolymer owns excellent ability of inhibiting or retarding the calcium deposits.

5. Conclusions

In summary, a non-phosphorus double-hydrophilic block copolymer AA-TPEL has been successfully synthesized by free radical polymerization and employed as an efficient scale inhibitor for CaCO_3 , CaSO_4 and $\text{Ca}_3(\text{PO}_4)_2$ scales. The polymer AA-TPEL gave around 88.67% efficiency for calcium carbonate at the pH (9.0) and temperature (80°C) with a 8 mg L^{-1} and exhibited 97.07% calcium sulfate inhibition efficiency only at a level of 3 mg L^{-1} under the condition of the pH (7.0) and temperature (70°C). AA-TPEL is also an effective $\text{Ca}_3(\text{PO}_4)_2$ inhibitor, and 98.92% inhibition efficiency was achieved only at a level of 4 mg L^{-1} under the condition of pH 7.0 and temperature 80°C .

Compared with commercial scale inhibitors PESA, HEDP and EDTMP, AA-TPEL showed an excellent inhibitory efficiency on calcium carbonate, calcium sulfate and carbonate phosphate precipitation. Structures of TPEG, TPEL and AA-TPEL were identified by FTIR and $^1\text{H NMR}$. SEM and XRD were applied to analyze the morphology and crystal structures. It indicated that the copolymer generated great impact on the morphology and crystal structures of CaCO_3 . As the concentration of copolymer increased to 8 mg L^{-1} , calcite was almost completely replaced by vaterite. The SEM and XRD studies for CaSO_4 revealed that the antiscalants dramatically changed the crystal habits or crystal morphology but the crystal structures were not much altered. The inhibition of $\text{Ca}_3(\text{PO}_4)_2$ deposit is mainly attributed to its superior dispersion performance of AA-TPEL.

Acknowledgments

This work was supported by the Prospective Joint Research Project of Jiangsu Province (BY2016076-01); the National Natural Science Foundation of China (51673040);

Scientific Innovation Research Foundation of College Graduate in Jiangsu Province (KYLX16_0266); a Project Funded by the Priority Academic Program Development of Jiangsu Higher Education Institutions (PAPD) (1107047002); the Fundamental Research Funds for the Central Universities (2242015k30001); Fund Project for Transformation of Scientific and Technological Achievements of Jiangsu Province of China (BA2016105); and Based on Teachers' scientific research SRTP of Southeast University (T16192003).

References

- [1] P. Shakkhivel, T. Vasudevan, Acrylic acid-diphenylamine sulphonic acid copolymer threshold inhibitor for sulphate and carbonate scales in cooling water systems, *Desalination*, 197 (2006) 179–189.
- [2] D. Hasson, H. Shemer, A. Sher, State of the art of friendly “green” scale control inhibitors: a review article, *Ind. Eng. Chem. Res.*, 50 (2011) 7601–7607.
- [3] H. Wang, G. Liu, J. Huang, Y. Zhou, Q. Yao, S. Ma, K. Cao, Y. Liu, W. Wu, W. Sun, Z. Hu, Performance of an environmentally friendly anti-scalant in CaSO_4 scale inhibition, *Desal. Wat. Treat.*, 53 (2013) 8–14.
- [4] M. Pons-Jiménez, R. Hernández-Altamirano, R. Cisneros-Dévora, E. Buenroostro-González, R. Oviedo-Roa, J.-M. Martínez-Magadán, L.S. Zamudio-Rivera, Theoretical and experimental insights into the control of calcium sulfate scales by using random copolymers based on itaconic acid, *Fuel*, 149 (2015) 66–77.
- [5] Y.M. Al-Roomi, K.F. Hussain, M. Al-Rifaie, Performance of inhibitors on CaCO_3 scale deposition in stainless steel & copper pipe surface, *Desalination*, 375 (2015) 138–148.
- [6] L. Ling, Y. Zhou, J. Huang, Q. Yao, G. Liu, P. Zhang, W. Sun, W. Wu, Carboxylate-terminated double-hydrophilic block copolymer as an effective and environmental inhibitor in cooling water systems, *Desalination*, 304 (2012) 33–40.
- [7] M. Dietzsch, M. Barz, T. Schuler, S. Klassen, M. Schreiber, M. Susewind, N. Loges, M. Lang, N. Hellmann, M. Fritz, K. Fischer, P. Theato, A. Kuhnle, M. Schmidt, R. Zentel, W. Tremel, PAA-PAMPS copolymers as an efficient tool to control CaCO_3 scale formation, *Langmuir*, 29 (2013) 3080–3088.
- [8] A.A. Al-Hamzah, C.P. East, W.O.S. Doherty, C.M. Fellows, Inhibition of homogenous formation of calcium carbonate by poly (acrylic acid). The effect of molar mass and end-group functionality, *Desalination*, 338 (2014) 93–105.
- [9] N. Mithil Kumar, S.K. Gupta, D. Jagadeesh, K. Kanny, F. Bux, Development of poly(aspartic acid-co-malic acid) composites for calcium carbonate and sulphate scale inhibition, *Environ. Technol.*, 36 (2015) 1281–1290.
- [10] H. Wang, Y. Zhou, Q. Yao, S. Ma, W. Wu, W. Sun, Synthesis of fluorescent-tagged scale inhibitor and evaluation of its calcium carbonate precipitation performance, *Desalination*, 340 (2014) 1–10.
- [11] Y. Bu, Y. Zhou, Q. Yao, Y. Chen, W. Sun, W. Wu, Inhibition of calcium carbonate and sulfate scales by a non-phosphorus terpolymer AA-APEY-AMPS, *Desal. Wat. Treat.*, 57 (2014) 1977–1987.
- [12] Y.M. Al-Roomi, K.F. Hussain, Application and evaluation of novel acrylic based CaSO_4 inhibitors for pipes, *Desalination*, 355 (2015) 33–44.
- [13] X. Liu, Z. Wang, Y. Zheng, S. Cui, M. Lan, H. Li, J. Zhu, X. Liang, Preparation, characterization and performances of powdered polycarboxylate superplasticizer with bulk polymerization, *Materials*, 7 (2014) 6169–6183.
- [14] Y. Li, C. Yang, Y. Zhang, J. Zheng, H. Guo, M. Lu, Study on dispersion, adsorption and flow retaining behaviors of cement mortars with TPEG-type polyether kind polycarboxylate superplasticizers, *Constr. Build. Mater.*, 64 (2014) 324–332.
- [15] L. Lei, J. Plank, A concept for a polycarboxylate superplasticizer possessing enhanced clay tolerance, *Cem. Concr. Res.*, 42 (2012) 1299–1306.

- [16] P. Shakkthivel, D. Ramesh, R. Sathiyamoorthi, T. Vasudevan, Water soluble copolymers for calcium carbonate and calcium sulphate scale control in cooling water systems, *J. Appl. Polym. Sci.*, 96 (2005) 1451–1459.
- [17] J.M. Marentette, J. Norwig, E. Stockelmann, W.H. Meyer, G. Wegner, Crystallization of CaCO_3 in the presence of PEO-block-PMAA copolymers, *Adv. Mater.*, 9 (1997) 647–651.
- [18] A.W. Xu, W.F. Dong, M. Antonietti, H. Cölfen, Polymorph switching of calcium carbonate crystals by polymer-controlled crystallization, *Adv. Funct. Mater.*, 18 (2008) 1307–1313.
- [19] H.K. Can, G. Üner, Water-soluble anhydride containing alternating copolymers as scale inhibitors, *Desalination*, 355 (2015) 225–232.
- [20] B. Guillemet, M. Faatz, F. Gröhn, G. Wegner, Y. Gnanou, Nanosized amorphous calcium carbonate stabilized by poly(ethylene oxide)-*b*-poly(acrylic acid) block copolymers, *Langmuir*, 22 (2006) 1875–1879.
- [21] C. Wang, S.-p. Li, T.D. Li, Calcium carbonate inhibition by a phosphonate-terminated poly(maleic-co-sulfonate) polymeric inhibitor, *Desalination*, 249 (2009) 1–4.
- [22] A. Antony, J.H. Low, S. Gray, A.E. Childress, P. Le-Clech, G. Leslie, Scale formation and control in high pressure membrane water treatment systems: a review, *J. Membr. Sci.*, 383 (2011) 1–16.
- [23] K. Cao, J. Huang, Y. Zhou, G. Liu, H. Wang, Q. Yao, Y. Liu, W. Sun, W. Wu, A multicarboxyl antiscalant for calcium phosphate and calcium carbonate deposits in cooling water systems, *Desal. Wat. Treat.*, 52 (2014) 7258–7264.
- [24] S. Patel, A.J. Nicol, Developing a cooling water inhibitor with multifunctional deposit control properties, *Mater. Perform.*, 35 (1996) 41–47.
- [25] K. Cao, Y. Zhou, G. Liu, H. Wang, W. Sun, Preparation and properties of a polyether-based polycarboxylate as an antiscalant for gypsum, *J. Appl. Polym. Sci.*, 131 (2014) 631–644.
- [26] B. Akın, M. Oner, Y. Bayram, K.D. Demadis, Effects of carboxylate-modified, “green” inulin biopolymers on the crystal growth of calcium oxalate, *Cryst. Growth Des.*, 8 (2008) 1997–2005.